Surface Science 606 (2012) 233–238

Contents lists available at SciVerse ScienceDirect

Surface Science

journal homepage: www.elsevier.com/locate/susc

Adsorption of water monomer and clusters on platinum(111) terrace and related steps and kinks II. Surface diffusion

Líney Árnadóttir [a], Eric M. Stuve [a,*], Hannes Jónsson [b]

[a] Department of Chemical Engineering, Box 351750, University of Washington, Seattle, WA 98195-1750, United States
[b] Faculty of Science, VR-II, University of Iceland, 107 Reykjavík, Iceland

ARTICLE INFO

Article history:
Received 29 June 2011
Accepted 28 September 2011
Available online 4 October 2011

Keywords:
Density functional theory
Water
Platinum
Terrace
Step surface
Kink surface
Adsorption
Diffusion

ABSTRACT

Surface diffusion of water monomer, dimer, and trimer on the (111) terrace, (221) and (322) stepped, and (763) and (854) kinked surfaces of platinum was studied by density functional theory using the PW91 approximation to the energy functional. Monomer diffusion on the terrace is facile, with an activation barrier of 0.20 eV, while dimer and trimer diffusions are restricted due to their high activation barriers of 0.43 and 0.48 eV, respectively. During monomer diffusion on the terrace the O–Pt distance increases by 0.54 Å, about 23% of the initial distance of 2.34 Å. The calculated rate of monomer diffusion hops is in good agreement with the onset temperature of diffusion measurements of Daschbach et al., J. Chem. Phys., 120 (2004) 1516. Alternative monomer diffusion pathways, in which the molecule rolls or flips, were also found. These pathways have diffusion barriers of 0.22 eV. During dimer diffusion on the terrace, the donor molecule rises 0.4 Å at the saddle point, while the acceptor rises by only 0.03 Å. Monomer diffusion up to steps and kinks, with activation barriers of 0.11–0.13 eV, facilitate chain formation on top of step edges. The energy landscape of monomer diffusion from terrace to step to kink sites is downhill with a maximum activation barrier of 0.26 eV. A model for water adsorption is presented in which monomer diffusion leads to concurrent formation of terrace clusters and population of steps/kinks, the latter consistent with the STM measurements of Morgenstern et al., Phys. Rev. Lett., 77 (1996) 703.

1. Introduction

Surface diffusion plays an important role in the early stages of water adsorption. On a surface composed of terrace and defect sites, initial adsorption of water occurs at terrace sites, as these outnumber defect sites. Monomeric water adsorbs weakly on late transition metals [1–6] and is stable as a monomer at temperatures of 40 K or less [7]. At higher temperature, experimental results show that surface diffusion leads to formation of larger clusters [8–11] and preferential adsorption at step edges relative to terrace sites [12,13].

Few calculations on water diffusion exist in the literature. Michaelides et al. [14] and Li et al. [15] both studied diffusion of water monomers on Al(100) and found the diffusion barrier to depend on path and orientation of the hydrogen atoms. Ranea et al. [16] calculated dimer diffusion via tunneling on Pd(111). They found agreement with the experimental findings of Salmeron et al. [8] that water dimer and trimer diffuse faster than water monomer on Pd(111).

As the mechanism of surface diffusion of water in the presence of defect sites is largely unknown, we used density functional theory (DFT) and the PW91 functional to examine diffusion barriers of water at terrace, step, and kink sites on a Pt(111) surface. The results provide a semi-quantitative description of surface diffusion through establishment of relative diffusion rates. Adsorption energies of water monomer and clusters on the (111) terrace, (221) and (322) step, and (763) and (854) kink sites were presented in a previous paper in this series [6]. In this paper we present pathways and activation energies for surface diffusion of water monomer on the aforementioned surfaces and for water dimer and trimer on the (111) terrace.

2. Methodology

Computational methods were described in the previous paper [6] and will be summarized here. All calculations were done with the Vienna ab-initio simulation package (VASP), a plane-wave implementation of DFT with the PW91 functional [17–21]. Interactions between ions and valence electrons were described by ultra-soft Vanderbilt pseudopotentials (US-PP) [22,23]. VASP supplies two US-PP for oxygen and hydrogen, and the harder potentials were used for both elements. A cut-off energy of 396 eV (29 Ry) was used for all the calculations; increasing the cut-off energy to 800 eV did not significantly affect the diffusion barrier. The hydrogen bond energy and bond length for a H_2O dimer in gas phase were calculated at various levels of theory, using PW91 and PBE functionals [24,25], PAW [26,27] and ultrasoft pseudopotentials, and varying the plane wave energy cutoff from

* Corresponding author. Tel.: +1 206 543 0156; fax: +1 206 543 3778.
E-mail addresses: lineya@u.washington.edu (L. Árnadóttir), stuve@u.washington.edu (E.M. Stuve), hj@hi.is (H. Jónsson).

0039-6028/$ – see front matter © 2011 Elsevier B.V. All rights reserved.
doi:10.1016/j.susc.2011.09.024

396 eV to 700 eV. The PW91/US-PP calculation with 396 eV cutoff gave a bond energy of 0.25 eV and a bond length of 2.86 Å, while a PBE/PAW calculation with 700 eV cutoff gave bond energy of 0.25 eV and bond length of 2.88 Å. The Brillouin zone was sampled with a $2\times2\times1$ Monkhorst-Pack k-point mesh per simulation cell. The calculations were considered converged when the maximum forces on all relaxed atoms were less than 50 meV/Å for adsorption on kinked and stepped surfaces and for nudged elastic band calculations; and 10 meV/Å for all other calculations. The rate and mechanism of water monomer and dimer diffusion on Pt(111) were determined by the climbing image, nudged elastic band (CI-NEB) method [28,29].

The calculated lattice constant for platinum was found to be 3.98 Å, and in good agreement with the experimental value of 3.924 Å [30]. The surface was cut out of a previously relaxed Pt-bulk and relaxed again keeping only the bottom layer fixed. Only the adsorbed molecules were allowed to relax during the calculations.

Structures of the five surfaces and most stable water configurations for water monomer and clusters were presented previously [6]. Calculations on the flat Pt(111) surface were performed with a total of 36 substrate atoms: 12 atoms per layer in three layers. Step sites were each represented by 12 and 15 surface atoms for type A and B steps, respectively. Kink sites A and B were represented by 14 and 12 surface atoms in 5 layers. Coordinates for the five surfaces and adsorbates can be found in the supplementary materials.

The (763) and (221) surfaces have (111)-oriented edges, which are referred to as type A steps and kinks. The (763) surface has (100)-oriented kinks. The (854) and (322) surfaces have (100)-oriented edges, which are referred to as type B steps and kinks. The (854) surface has (111)-oriented kinks.

An onset temperature of diffusion was determined from a diffusion rate constant k calculated with quasi-quantum harmonic transition state theory (qq-hTST) [31,32], where quantum mechanical partition functions (Q_{qm}) are used for vibrational modes defined from the classical equations of motion Eq. (1). The qm-hTST includes no tunneling and should therefore approach the classical hTST at infinite temperature.

$$k_{qm} = \frac{2k_BT}{h}\frac{\prod_i^N \sinh\left(h\nu_i^R/2k_BT\right)}{\prod_i^{N-1} \sinh\left(h\nu_i^{\ddagger}/2k_BT\right)} exp\left(\frac{-\Delta E}{k_BT}\right) \quad (1)$$

where N is the number of vibrational modes in the initial configuration, $\nu_{i,R}$ the vibrational frequencies of the initial configuration (reactant, R), $\nu_i^{\ddagger}$ the vibrational frequencies at the saddle point, and

$$\Delta E = E^{\ddagger} - E_R, \quad (2)$$

with $E^{\ddagger}$ as the energy at the saddle point and E_R as the energy minimum of the initial configuration. The frequencies ν_i of the vibrational modes were calculated classically from the eigenvalues of the Hessian matrix, which was constructed using finite differences with displacements of 0.01 Å.

3. Results

3.1. Terrace diffusion

Diffusion of monomer, dimer, and trimer from one atop site to another on a Pt(111) terrace was studied with the CI-NEB method. The minimum energy path (MEP) for monomer diffusion is shown in Fig. 1. Eighteen images were calculated for this path. The energy barrier and location of the saddle point were insensitive to the number of images for this path for 7 images or more. At the saddle point water is positioned over a bridge site with its molecular plane twisted 12° about an axis approximately parallel to the surface plane. The saddle point is

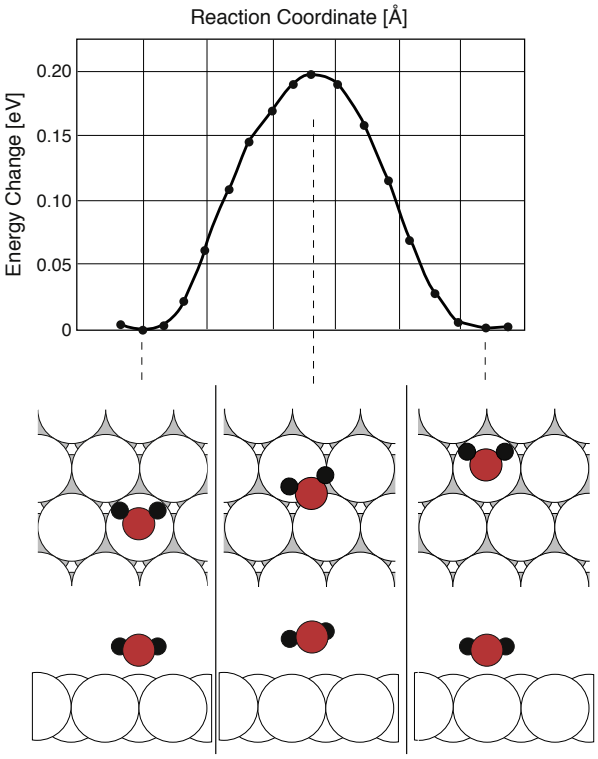

Fig. 1. Monomer diffusion on Pt(111); the diffusion barrier is 0.20 eV. The lower figures show configurations of the initial (left), saddle (center), and final (right) points of diffusion.

0.20 eV higher in energy than the initial/final states and equidistant from them. This is much larger than a previously reported estimate of 0.03 eV based on semi-empirical calculations [33]. It is interesting to note that this diffusion activation energy is similar to an estimated value for the average diffusion activation energy of a water molecule on an ice Ih surface [34].

Fig. 2a shows another diffusion path, a rolling path, where the hydrogen atoms in the final state point in the opposite direction as in the initial state. The rolling path has a slightly higher energy barrier of 0.22 eV. The first half of the MEP looks the same as the non-rolling pathway, but just before the saddle point the molecule rolls over with the hydrogen atoms directed away from the surface. Fig. 2b shows a third diffusion path, where the water molecule flips over with the hydrogen atoms directed towards the surface. This path also has an energy barrier of 0.22 eV. Similar diffusion paths were investigated earlier on Al(100) and Pd(111) [15,35].

Three snapshots of the minimum energy path for dimer diffusion are shown in Fig. 3: initial configuration, saddle point, and final configuration. Hydrogen bond donor molecules are identified with the plus (+) sign and acceptor molecules with no sign.

The energy barrier for dimer diffusion is 0.43 eV. The height of the acceptor molecule, determined by the oxygen height above the Pt surface, changes by only 0.03 Å during diffusion, although the donor molecule shifts up by 0.39 Å. Diffusion barriers and O–Pt distances for water monomer and dimer are shown in Table 1. In diffusion on the terrace, the monomer and the donor molecule of the dimer are displaced from their most stable distance by 0.54 and 0.39 Å, respectively, and the monomer diffusion barrier is less than half that of the dimer.

A summary of forward and reverse barriers, energy change, and nset temperatures of diffusion is given in Table 2 for all of the cases studied here. The forward direction of diffusion was chosen to be from

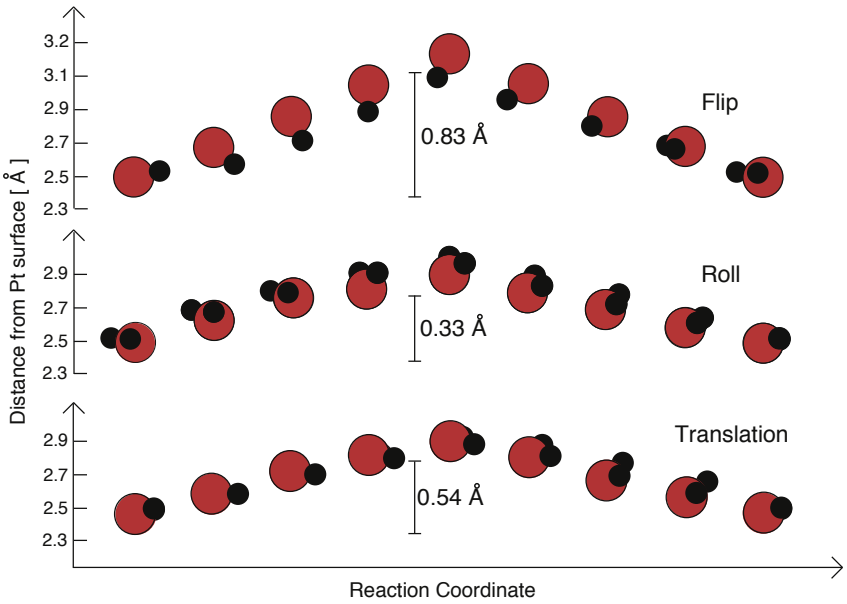

Fig. 2. Flipping, rolling and translational diffusion of water monomer on Pt(111). The flipping diffusion begins as in Fig. 1, but the molecule rolls over pointing the hydrogen atoms in the opposite direction in the final state relative to the initial state. The rolling path is similar except that the hydrogen atoms point away from the surface during diffusion. In all cases diffusion is between a nearest neighbor platinum atom atop sites. The diffusion height over the Pt(111) surface is shown on the y-axis.

higher energy to lower energy. Each diffusion process is labeled with a path number depicted in Fig. **4**.

Monomer, dimer, and trimer diffusion on the terrace are labeled D_1, D_2, and D_3, respectively. The activation barrier for diffusion increases from 0.20 eV for the monomer to 0.48 eV for the trimer. Thus, larger clusters diffuse more slowly than monomers. In contrast, dimers were found to diffuse faster than monomers on the Pd(111) surface [8,16]. We will discuss this further in Section **4**.

3.2. Diffusion on and up to steps and kinks

Activation barriers for diffusion and adsorption energies on steps and kinks are summarized in Table **2** and show that the energy difference between two different adsorption sites is often substantial. Consequently, the forward and reverse activation barriers can be significantly different. Fig. **4** illustrates monomer diffusion onto and along type A and type B steps and kinks. Diffusion at steps is relatively facile, as forward activation barriers are in the range of 0.066 to 0.16 eV, except for path D_5, which has a forward barrier of 0.22 eV, still conducive to diffusion. The barriers for diffusion from the lower terrace onto the step edge are relatively low, 0.066 eV for step-A (D_4) and 0.13 eV for step-B (D_6), indicating that water readily diffuses from the lower terrace to the step edge. Once there, the tendency to diffuse away is lower, as seen by the relatively large reverse activation barriers of 0.31 eV for step A (D_{-4}) and 0.34 eV for step B (D_{-6}), respectively. (The minus signs indicate reverse diffusion paths.) Similarly, diffusion

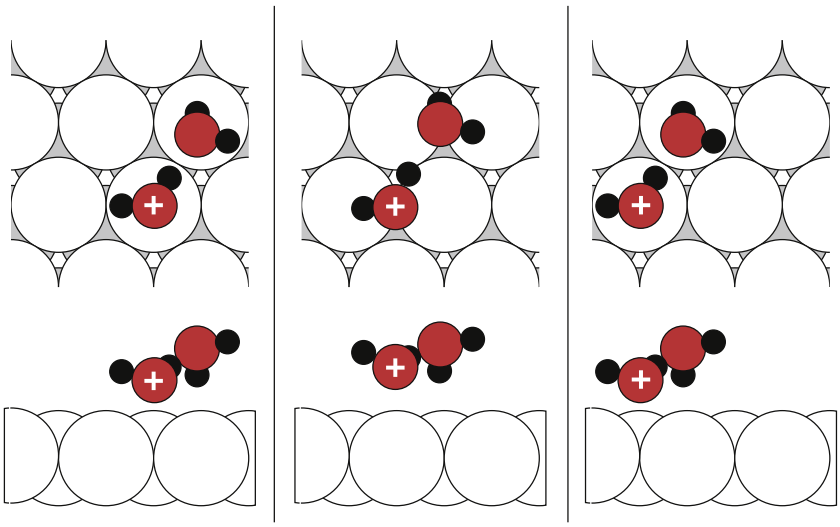

Fig. 3. Dimer diffusion on Pt(111); the diffusion barrier is 0.43 eV. Top and side views are shown for the initial configuration (left), saddle point (center), and final configuration (right). The white cross designates the donor molecule. Note that the donor molecule moves significantly away from the surface at the saddle point, while the acceptor molecule remains at nearly the same distance from the surface throughout the process.

Table 1
Diffusion barrier, initial state O–Pt distance O–Pt_{init}, and change in O–Pt distance Δ(O–Pt) of the saddle configuration relative to the initial configuration.

Species	E_a [eV]	O–Pt_{init} [Å]	Δ(O–Pt) [Å]
Monomer			
Translation	0.20	2.34	0.54
Roll	0.22	2.37	0.33
Flip	0.22	2.37	0.83
Dimer	0.43		
Donor		2.24	0.39
Acceptor		3.18	0.03

from the upper terrace to the step edge (D_8) is also favored, while the reverse process (D_{-8}), with a barrier of 0.43 eV, is strongly disfavored.

The step edge affects the adsorption energy of water on the lower terrace near the step edge. Water adsorbed near step A (the initial state in path D_4) is 0.08 eV weaker bound than water on a Pt(111) terrace. Equivalent values for water near step B and kinks A and B are listed in Table **2** and range from 0.22 to 0.27 eV.

Water diffusion to a kink atom (paths D_9 through D_{13}) is slightly more hindered than for step sites; diffusion barriers range from 0.13 to 0.26 eV—still conducive for diffusion at liquid nitrogen temperatures, as discussed in Section 3.3. As in the case for diffusion at steps, once water is at the kink atom, it has little tendency to diffuse away, as reverse activation barriers (D_{-9}–D_{-13}) range from 0.34 to 0.48 eV. It is interesting to note that diffusion from the kink atom to a step edge (D_{-10} and D_{-12}) is also disfavored.

Fig. **5** shows the energy landscape for monomer diffusion from the terrace up to the step edge and along the step edge to the kink site. The energy on the terrace is set to zero. Diffusion up to a type A step and kink is shown in the black (solid) line and diffusion up to a type B step and kink is shown in the red (dashed) line. The diffusion pathway for water monomer is downhill from terrace to kink site, with the largest activation barriers (0.23 and 0.26 eV for types A and B, respectively) being for the last step, from step edge to kink atom. The heat of adsorption of the final state at the kink site is greater than that of the initial state energy at the terrace site by 0.35 and 0.39 eV for the A and B kinks, respectively.

3.3. Onset temperature of diffusion

The onset temperature of diffusion, defined as the temperature that produces an average time of one second between hops ($\tau = 1\ s^{-1}$), was calculated with quasi-quantum harmonic transition state theory, Eq. (1), and are shown as T_{diff} in Table **2**. The prefactor was evaluated from the calculated vibrational frequencies for the monomer translation and was found to be $5 \times 10^{15}\ s^{-1}$. Together with the activation barrier of 0.20 eV, the onset temperature comes out to be 64 K. The one-second hopping time was somewhat arbitrarily chosen, though the relative trends among different diffusion paths will be insensitive to the choice of hopping time. The rolling and the flipping diffusion pathways do not have the same initial and finial state as the translational pathway and can therefore be considered as different elementary steps. However, rotation of the monomer around its z-axis on the atop site has little to no barrier [6] making the three diffusional pathways accessible. Inclusion of these three pathways decreases the onset temperature to 62 K.

The calculated onset temperature for monomer diffusion is in reasonably good agreement with the experimental value of 60 K obtained by helium scattering experiments on Pt(111) by Daschbach, et al. [10]. In contrast, the high activation barrier for dimer diffusion of 0.43 eV translates to a high onset temperature of 155 K, close to the desorption temperature of water. The high activation barrier may be a consequence of the deformation required for dimer diffusion, as shown in Fig. **3**. The onset temperature of trimer diffusion of 174 K is even higher by virtue of its higher activation barrier of 0.48 eV. Thus, diffusion and cluster formation on the terrace proceed by two monomers combining to form a dimer, which is essentially immobile. These clusters can then grow by further attachment of monomers.

All other steps listed in Table **2** have relatively low diffusion temperatures, at least in the forward direction. The forward activation barriers of all step and kink diffusion paths are 0.26 eV or less. Diffusion paths D_4 through D_{13} should be facile at temperatures of 100 K or less.

Table. 2
Diffusion path, forward activation barrier $E_{a,f}$, reverse activation barrier $E_{a,r}$, path energy change $-\Delta E$, adsorption energy of initial site $E_{a,ads}$ and onset temperature of diffusion T_{diff} for water diffusion on terrace, steps, and kinks. Monomer, dimer, and trimer water are signified by M, D, and T, respectively.

Path	Type	$E_{a,f}$ [eV]	$E_{a,r}$ [eV]	$-\Delta E$ [eV]	$E_{a,ads}$ [eV]	T_{diff} [K]
D_1	Terrace-M	0.20	0.20	0	0.30	64
D_2	Terrace-D	0.43	0.43	0	0.45	155
D_3	Terrace-T	0.48	0.48	0	0.48	174
D_4	Step-A	0.066	0.31	0.24	0.22	10
D_5	Step-A	0.22	0.22	0	0.47	72
D_6	Step-B	0.13	0.34	0.21	0.26	35
D_7	Step-B	0.16	0.16	0	0.46	48
D_8	Step-B	0.11	0.43	0.32	0.22	27
D_9	Kink-A	0.13	0.43	0.30	0.24	35
D_{10}	Kink-A	0.23	0.34	0.11	0.43	76
D_{11}	Kink-B	0.13	0.47	0.34	0.23	35
D_{12}	Kink-B	0.26	0.44	0.18	0.39	88
D_{13}	Kink-B	0.20	0.37	0.17	0.40	64

4. Discussion

The energy landscape that emerges from these calculations can be used to construct a model for water cluster formation on the Pt(111) surface. Water molecules adsorbed on the flat terrace will diffuse to step sites, with little tendency to diffuse away from them. This continues until the step is fully populated. Diffusion along step edges is facile, thereby enabling extended, one-dimensional configurations to form. At full population the lowest energy configuration of water on steps A and B is a zigzag extended configuration with per-molecule adsorption energies of 0.57 and 0.55 eV, respectively [6].

An interesting result is the high diffusion barrier of the terrace dimer relative to the monomer, especially in comparison to dimer diffusion on Pd(111) [8,16]. In the latter case dimer diffusion was found to be more facile than monomer diffusion; the activation barrier for dimer diffusion was just 0.13 eV [8]. The mechanism for enhanced dimer diffusion rates has been attributed to a hydrogen bond donor–acceptor tunneling exchange, in which the transition state is entropically stabilized by the alternating donor–acceptor complex [16].

The case for Pt(111) is distinct from that for Pd(111), as several experimental studies support slower dimer diffusion relative to monomer diffusion. Helium atom diffraction studies by Glebov et al. [7] and Daschbach et al. [10] show that water monomer becomes mobile at 40–60 K, above which clusters are formed. The clusters remain stable, eventually forming a wetting layer at temperatures in the range of 100–140 K. Infrared reflection–absorption spectroscopy by Ogasawara et al. [36,37] suggest that monomers are stable below 40 K and at higher temperature cluster to form a wetting layer. This was initially interpreted to be bilayer ice, but has more recently been shown by Nie et al. [38] to be a combination of 5 and 7 water molecule rings.

As to the difference between Pd(111) and Pt(111), we note that the alternating donor/acceptor complex on Pd(111) requires both

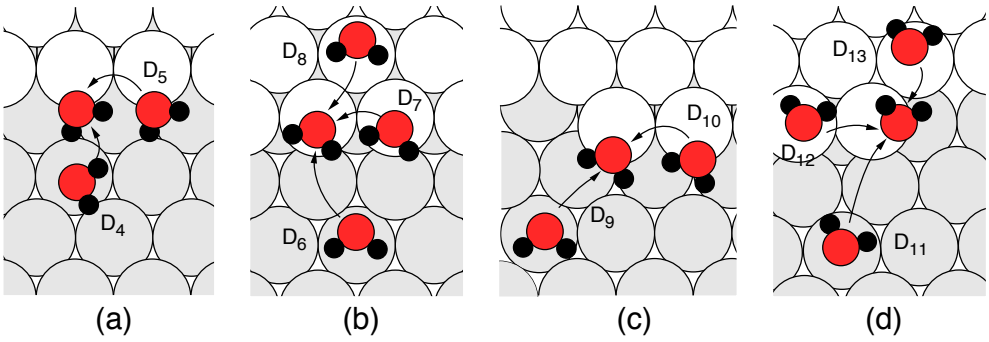

Fig. 4. Diffusion up to and along step A (a), step B (b), kink A (c), and kink B (d). In these views the surface is tilted slightly away from [111] to show detail at the step and kink sites. Activation energies and energy changes for the individual diffusion paths are listed in Table 2.

water molecules to be strongly bonded to the metal at the saddle point [39]. The acceptor molecule, weakly bonded in the initial state, must bond more strongly at the saddle point. The weaker metal–water bonding on Pt(111) [6] relative to Pd(111) acts against strong adsorption of the acceptor molecule. Hence, the driving force for forming the alternating donor/acceptor complex is less for Pt(111) to the extent that faster dimer diffusion via the mechanism proposed by Mitsui et al. [8], does not occur.

The DFT calculations discussed here support the following mechanism for water adsorption and desorption. Because of the large area of terrace sites, water will adsorb first as a monomer, then diffuse rapidly to step sites, and then to kink sites. Once the kink sites are saturated, step sites will begin to fill with water in a zigzag, extended configuration [5,6]. Once the step sites are saturated, terrace sites will begin to fill. If, during the adsorption process, two monomers form a dimer on the terrace, an immobile cluster will be formed that can grow through addition of monomers at the cluster edge. In this case, adsorption at immobile terrace clusters occurs concurrently with population of steps. The relative extents of these processes will depend on the relationship of incident flux of water from the gas phase and substrate temperature, which controls the diffusion processes. Along this line, Daschbach et al. [10] studied the influence of incident flux on water adsorption on Pt(111). They found no dependence on flux over the range of 0.005–0.55 ML s^{-1}. Therefore, a test of the adsorption mechanism proposed here will require incident fluxes greater than 0.55 ML s^{-1}.

Water desorption proceeds, by microscopic reversibility, in the reverse manner. Terrace molecules desorb first, followed by migration from step sites to the terrace and then desorption, followed by migration from kink sites to step sites to the terrace and then desorption.

5. Conclusions

DFT calculations were used to determine activation energies for surface diffusion of water monomers and small clusters on Pt(111) terrace, (221) and (322) steps, and (763) and (854) kink sites.

Monomer diffusion along a terrace occurs with an increase in the O–Pt distance of 0.54 Å, or 23% of its initial distance of 2.34 Å. The activation energy for this process is 0.20 eV. Alternative diffusion paths, in which the molecule rolls/flips at the transition state directing the hydrogen atoms away/towards the surface, have slightly higher activation energies of 0.22 eV for both paths. Dimer diffusion on the terrace leads to an increase of the O–Pt distance of 0.39 Å for the donor molecule, but only 0.03 Å for the acceptor molecule. The dimer diffusion barrier of 0.43 eV is relatively large, more than twice that of the monomer, implying that dimer diffusion will be inactive for temperatures up to the desorption temperature of water.

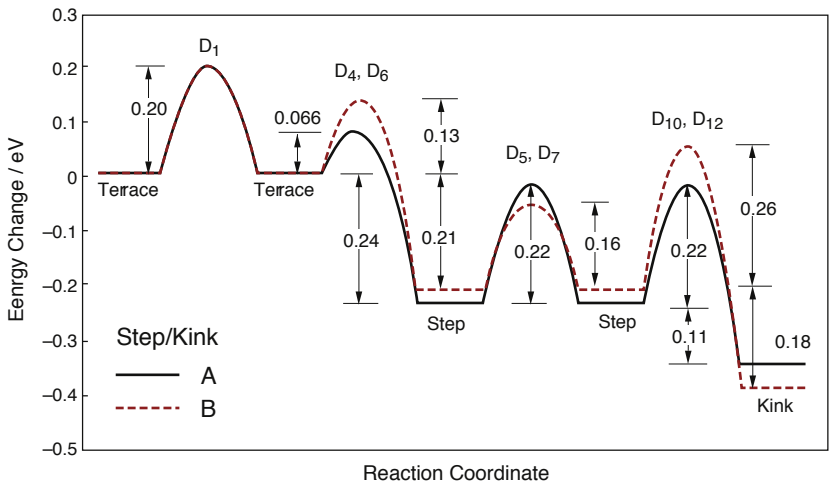

Fig. 5. Energy landscape for monomer diffusion from the flat terrace up to step A and along the step edge to a kink site shown in black (solid) lines. The same path from the flat terrace up to and along step B is shown in red (dashed) lines.

The energy landscape for monomer diffusion on Pt(111) and type A [(221) and (763)] and type B [(322) and (854)] step and kink surfaces shows that monomer diffusion proceeds along the terrace, up to the step edge, and along the edge to a kink site (or from terrace to kink site directly). The highest activation barrier for this diffusion process is 0.26 eV, suggesting that at low temperatures (about 100 K) water will diffuse up to steps and kinks and form chains on the step edges before wetting the lower terrace, in good agreement with experimental findings [13].

From the combined adsorption and diffusion results we developed a phenomenological model of water adsorption. In the first step water adsorbs as a monomer and diffuses rapidly to a step or terrace cluster. Monomers at step sites will diffuse to kink sites until fully populated, and remaining molecules will diffuse to form predominantly zigzag chains until full population of step sites. Terrace clusters form by monomers combining to produce dimers, which are essentially immobile, and cluster growth proceeds by subsequent addition of monomers.

Acknowledgments

Major funding for this work was provided by the Office of Naval Research, the National Science Foundation and EC MC-RTN Hydrogen. A portion of the research was performed as part of an EMSL Scientific Grand Challenge project at the W. R. Wiley Environmental Molecular Sciences Laboratory, a national scientific user facility sponsored by the U.S. Department of Energy's Office of Biological and Environmental Research and located at the Pacific Northwest National Laboratory. The Pacific Northwest National Laboratory is operated for the Department of Energy by Battelle.

Appendix A. Supplementary data

Supplementary data to this article can be found online at doi:10.1016/j.susc.2011.09.024.

References

[1] P.A. Thiel, T.E. Madey, Surf. Sci. Rep. 7 (1987) 211.
[2] M.A. Henderson, Surf. Sci. Rep. 46 (2002) 5.
[3] A. Hodgson, S. Haq, Surf. Sci. Rep. 64 (2009) 381.
[4] A. Michaelides, V.A. Ranea, P.L. de Andres, D.A. King, Phys. Rev. Lett. 90 (2003) 216102.
[5] S. Meng, E.G. Wang, S.W. Gao, Phys. Rev. B 69 (2004) 195404.
[6] L. Árnadóttir, H. Jónsson, E. Stuve, Surf. Sci. 602 (2010) 1978.
[7] A.L. Glebov, A.P. Graham, A. Menzel, Surf. Sci. 427-428 (1999) 22.
[8] T. Mitsui, M.K. Rose, E. Fomin, D.F. Ogletree, M. Salmeron, Science 297 (2002) 1850.
[9] K. Morgenstern, J. Nieminen, Phys. Rev. Lett. 88 (2002) 066102.
[10] J.L. Daschbach, B.M. Peden, R.S. Smith, B.D. Kay, J. Chem. Phys. 120 (2004) 1516.
[11] K. Motobayashi, C. Matsumoto, Y. Kim, M. Kawai, Surf. Sci. 602 (2008) 3136.
[12] K. Morgenstern, Surf. Sci. 504 (2002) 293.
[13] M. Morgenstern, T. Michely, G. Comsa, Phys. Rev. Lett. 77 (1996) 703.
[14] A. Michaelides, A. Alavi, D.A. King, Phys. Rev. B 69 (2004) 113404.
[15] J.B. Li, Y. Li, S.L. Zhu, F.H. Wang, Phys. Rev. B 74 (2006) 153415.
[16] V.A. Ranea, A. Michaelides, R. Ramirez, P.L. de Andres, J.A. Verges, D.A. King, Phys. Rev. Lett. 92 (2004) 136104.
[17] G. Kresse, J. Hafner, Phys. Rev. B 47 (1993) 558.
[18] G. Kresse, J. Hafner, Phys. Rev. B 49 (1994) 14251.
[19] G. Kresse, J. Furthmuller, Comput. Mater. Sci. 6 (1996) 15.
[20] G. Kresse, J. Furthmuller, Phys. Rev. B 54 (1996) 11169.
[21] J.P. Perdew, Y. Wang, Phys. Rev. B 45 (1992) 13244.
[22] D. Vanderbilt, Phys. Rev. B 41 (1990) 7892.
[23] G. Kresse, J. Hafner, J. Phys.-Condens. Matter 6 (1994) 8245.
[24] J.P. Perdew, K. Burke, M. Ernzerhof, Phys. Rev. Lett. 77 (1996) 3865.
[25] J.P. Perdew, K. Burke, M. Ernzerhof, Phys. Rev. Lett. 78 (1997) 1396.
[26] P. Blochl, Phys. Rev. B 50 (1994) 17953.
[27] G. Kresse, D. Joubert, Phys. Rev. B 59 (1999) 1758.
[28] G. Henkelman, B.P. Uberuaga, H. Jonsson, J. Chem. Phys. 113 (2000) 9901.
[29] G. Henkelman, H. Jónsson, J. Chem. Phys. 113 (2000) 9978.
[30] Handbook of Chemistry and Physics, in: D. Lide (Ed.), 78 ed., CRC Press, Inc., New York, 1997–1998.
[31] A. Arnaldsson, Ph.D. thesis, University of Washington, 2007.
[32] G. Henkelman, A. Arnaldsson, H. Jonsson, J. Chem. Phys. 124 (2006) 044706.
[33] A.B. Anderson, Surf. Sci. 105 (1981) 159.
[34] E.R. Batista, H. Jónsson, Comput. Mater. Sci. 20 (2001) 325.
[35] J.B. Li, S.L. Zhu, Y. Li, F.H. Wang, J. Am. Chem. Soc. 130 (2008) 11140.
[36] H. Ogasawara, J. Yoshinobu, M. Kawai, J. Chem. Phys. 111 (1999) 7003.
[37] H. Ogasawara, B. Brena, D. Nordlund, M. Nyberg, A. Pelmenschikov, L.G.M. Pettersson, A. Nilsson, Phys. Rev. Lett. 89 (2002) 276102.
[38] S. Nie, P.J. Feibelman, N.C. Bartelt, K. Thuermer, Phys. Rev. Lett. 105 (2010) 026102.
[39] A. Michaelides, Appl. Phys. A-Mater. Sci. Process. 85 (2006) 415.